The Journal of Chemical Physics

All-atom molecular dynamics study on the non-solvent induced phase separation: Thermodynamics of adding water to poly(vinylidene fluoride)/*N*-methyl-2-pyrrolidone solution

Cite as: J. Chem. Phys. **150**, 184505 (2019); https://doi.org/10.1063/1.5094088
Submitted: 27 February 2019 . Accepted: 25 April 2019 . Published Online: 14 May 2019

Tseden Taddese, Masahiro Kitabata, and Susumu Okazaki

The Journal of Chemical Physics ARTICLE scitation.org/journal/jcp

All-atom molecular dynamics study on the non-solvent induced phase separation: Thermodynamics of adding water to poly(vinylidene fluoride)/*N*-methyl-2-pyrrolidone solution

Cite as: J. Chem. Phys. 150, 184505 (2019); doi: 10.1063/1.5094088
Submitted: 27 February 2019 • Accepted: 25 April 2019 •
Published Online: 14 May 2019

Tseden Taddese,[1] Masahiro Kitabata,[1,2,3] and Susumu Okazaki[1,a)]

AFFILIATIONS

[1] Department of Materials Chemistry, Graduate School of Engineering, Nagoya University, Furo-Cho, Chikusa-Ku, Nagoya, Aichi 464-8603, Japan
[2] Research Association of High-Throughput Design and Development for Advanced Functional Materials (ADMAT), 2266-98 Anagahora, Shimo-Shidami, Moriyama-Ku, Nagoya, Aichi 463-8560, Japan
[3] Advanced Materials Research Laboratories, Toray Industries, Inc., 2-1 Sonoyama 3-Chome, Otsu, Shiga 520-0842, Japan

[a)] **Author to whom correspondence should be addressed:** okazaki@chembio.nagoya-u.ac.jp

ABSTRACT

The change in the thermodynamics when adding water in poly(vinylidene fluoride) (PVDF)/*N*-methyl-2-pyrrolidone (NMP) solution is studied from all atom molecular dynamics (MD) simulations. This is done by estimating the free energy of mixing of PVDF/NMP solution with increasing volume fraction of water (ϕ_w) using an appropriately chosen thermodynamic cycle and the Bennett acceptance ratio method. The MD calculations predict the thermodynamic phase separation point of water/NMP/PVDF to be at $\phi_w = 0.08$, in close agreement with the experimental cloud point measurement ($\phi_w = 0.05$). Examining the enthalpic and entropic components of the free energy of mixing reveals that at low concentrations of water, the enthalpy term has the most significant contribution to the miscibility of the ternary system, whereas at higher concentrations of water, the entropy term dominates. Finally, the free energy of mixing was compared with the Flory-Huggins (FH) free energy of mixing by computing the concentration-dependent interaction parameters from MD simulations. The FH model inadequately predicted the miscibility of the PVDF solution, mainly due to its negligence of the excess entropy of mixing.

INTRODUCTION

Predicting the miscibility of nonsolvent/solvent/polymer systems is important for the polymeric membrane production. In particular, the nonsolvent induced phase separation (NIPS) method involves immersing a homogeneous polymer solution in a nonsolvent bath, where solvent exchange occurs. This leads to solid-liquid phase separation of the solution due to precipitation of the polymer and results in the formation of polymeric membranes with particular morphological properties.[1] Information about the miscibility of the nonsolvent/solvent/polymer system is required to control such membrane morphology through appropriate solvent selection and control of polymer phase separation. It is widely accepted that these morphological characteristics strongly depend on both the thermodynamic and the kinetic aspects of the membrane forming system.[2–4] In this work, we focus on the equilibrium thermodynamics phase behavior of nonsolvent/solvent/polymer systems, which represents the first step toward predicting their miscibility.

Thermodynamic analysis of the phase behavior of nonsolvent/solvent/polymer ternary systems can be carried out

experimentally through cloud point measurements, which correspond to the binodal line, the boundary between the homogeneous mixture and two-phase regions. On the other hand, Tompa's extension[5] of the classical Flory-Huggins (FH)[6,7] model (mean-field description based on a lattice model) can be applied to estimate the theoretical miscibility of such ternary systems by calculating the free energy of mixing, ΔG_m^{FH}, as

$$\Delta G_m^{FH} = RT[n_1 \ln \phi_1 + n_2 \ln \phi_2 + n_3 \ln \phi_3 + \chi_{12}(u_2) n_1 \phi_2 + \chi_{13}(\phi_3) n_1 \phi_3 + \chi_{23}(\phi_3) n_2 \phi_3]. \quad (1)$$

The subscripts above refer to nonsolvent (1), solvent (2), and polymer (3), with n_i and ϕ_i, respectively, corresponding to the number of moles and the volume fraction of species i and $u_2 = \phi_2/(\phi_1 + \phi_2)$. The gas constant is denoted R, and the temperature of the system is denoted T. Within the FH theory, the interaction parameter χ_{ij} is a dimensionless parameter that describes the difference in the strength of the pairwise interaction energies between components i and j in a mixture, compared with the same components in a pure state. Negative values of χ_{ij} represent systems that promote mixing, e.g., a polymer in a good solvent, whereas positive values mean the system favors phase separation, e.g., a polymer in a nonsolvent. This is a simple method that assumes that the ternary system behavior can be described using pairwise addition of binary contributions. It ignores the connectivity of the polymer chain, as well as the conformational entropy. In most studies, the value of χ_{13} and χ_{23} are taken as constant values even though it is well understood that χ_{ij} depends on the concentration of each component.[8] In some cases, χ_{13} is simply taken as a fitting parameter to match cloud point experimental measurements. This theory, despite its major simplifying assumptions, has been widely applied to predict the miscibility of polymers with other small compounds in many different research fields, such as in food polymer science[9] and drug formulation.[10] Within polymer membrane studies, the FH model is applied in mesoscopic simulations of the NIPS process.[11,12] However, the basic method has recently been shown to be inadequate when trying to predict the compatibility of polymers with small compounds, e.g., polymer-drug interactions,[13,14] and with other polymers.[15–17] This is due to inaccurate estimation of χ_{ij} and subsequently of ΔG_m. Therefore, there is a great need to adopt a more accurate scheme for calculating ΔG_m, which does not rely on the FH theory, in order to make a quantitative prediction of the thermodynamic properties of nonsolvent/solvent/polymer systems.

Molecular dynamics (MD) simulation can be employed to gain molecular level insight into the miscibility of various systems. Within MD simulation, extensive work in the last 30 years has led to the development of free energy calculation methods for various physical processes, which have been shown to be fairly accurate.[18–20] These methods have been widely applied to determine solvation and binding free energies,[21,22] but very little work has been done to estimate free energy of mixing. Recent work by Jedlovszky *et al.*[23] had shown that the free energy of mixing of various compositions of water and acetone can be accurately estimated through computer simulation using the method of thermodynamic integration (TI). They demonstrated that TI calculations can determine whether a given binary system is thermodynamically stable. Following the same methodology, Idrissi *et al.*[24] estimated the free energy of mixing of water with dimethyl sulfoxide (DMSO) over the entire composition range, in close agreement with experimental results, shedding some light on the miscibility of water and DMSO. However, to the best of our knowledge, there is no existing literature that calculates ΔG_m of nonsolvent/solvent/polymer systems from MD calculation.

In this work, we perform all-atom MD simulations to predict the thermodynamic phase behavior of water/*N*-methyl-2-pyrrolidone (NMP)/poly(vinylidene fluoride) (PVDF) system from free energy of mixing calculations, denoted ΔG_m^{MD}. We chose this system since semicrystalline PVDF is commonly used as a polymeric membrane due to its high thermal stability, high chemical resistance, and suitable processability. Moreover, the hydrophobic nature of PVDF is advantageous as it allows water to be used as the nonsolvent in the NIPS process, greatly reducing the cost, and a PVDF solution can easily be prepared with common organic solvents such as NMP.

Here, we show from the MD calculations that the predicted phase transition point of water/NMP/PVDF (from homogeneous to a two-phase system) is close to the experimental cloud point measurement. Furthermore, we compare the ΔG_m^{MD} calculation results with the theoretical value, ΔG_m^{FH}, estimated by applying the concentration dependence of all χ_{ij} from MD simulations. The comparison clearly shows that the FH theory is unsatisfactory and could be improved numerically making use of its functional form.

METHODOLOGY

Free energy of mixing from MD calculation

The following is a description of the procedure to calculate the free energy of mixing of the PVDF solution with water, from MD simulations. First, let us denote the PVDF/NMP system (with N_P being the number of PVDF molecules and N_N being the number of NMP molecules) as $S_{N/P}$, with corresponding free energy $G_{N/P}$, and a pure water system as S_w with free energy G_w. The change in the free energy, ΔG_m, upon adding water into the PVDF/NMP system, resulting in a water/NMP/PVDF ternary system (S_m with free energy G_m), is given by

$$\Delta G_m = G_m - \left(x_w G_w + x_{N/P} G_{N/P}\right), \quad (2)$$

where $x_{N/P} = x_{NMP} + x_{PVDF}$ represents the mole fraction of the PVDF/NMP system and $x_w = x_{water}$ represents the mole fraction of the water system. We cannot use MD simulation ensembles to calculate the right-hand side of Eq. (2) directly due to the difficulty in quantifying the exact free energy of a system because of insufficient sampling during finite length simulations. However, it is possible to compute free energy differences between two closely related states of a given system based on standard free energy calculation techniques such as TI and the Bennett Acceptance Ratio (BAR) methods.[25] In particular, the free energy associated with the process of adding water from bulk into the PVDF solution can be analyzed from MD simulations using the thermodynamic cycle shown in Fig. 1, where water in a gas state (g) is taken as the reference state.

In this work, the BAR method[25] is implemented to quantify the value of $\Delta G_{w(g \to S_w)}$ and $\Delta G_{w(g \to S_w)}$ when adding ΔN_w water molecules. Following the thermodynamic cycle and considering the

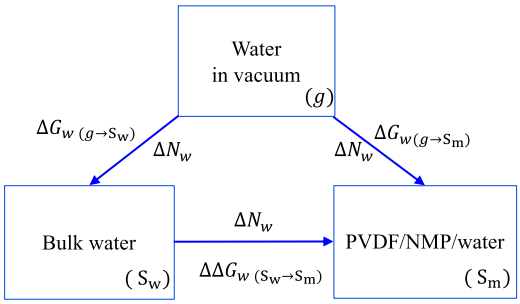

FIG. 1. The thermodynamic cycle showing the free energy change $\Delta\Delta G_{w(S_w\to S_m)}$ upon inserting water molecules from bulk of water (S_w) into the PVDF solution (S_m). The values of $\Delta G_{w(g\to S_w)}$ and $\Delta G_{w(g\to S_m)}$ correspond to the free energy change upon adding ΔN_w water molecules from the gas state (g) to systems S_w and S_m, respectively.

mixing process as a sequence of stepwise additions of the same amount of water, ΔN_w, at each stage, the free energy of adding water from the gas state (g) into system S_w at step i is taken as

$$\Delta G_{w(g\to S_w)}((i+1)\Delta N_w) = G_w((i+1)\Delta N_w) - \left(G_w(i\Delta N_w) + G_w^g(\Delta N_w)\right). \quad (3)$$

Similarly, the free energy of adding water from the gas state into S_m at step i is

$$\Delta G_{w(g\to S_m)}((i+1)\Delta N_w) = G_m(N_P, N_N, (i+1)\Delta N_w) - \left(G_m(N_P, N_N, i\Delta N_w) + G_w^g(\Delta N_w)\right), \quad (4)$$

where G_m refers to the free energy of the water/NMP/PVDF system (S_m), G_w refers to the bulk water system (S_w), and G_w^g refers to the water molecules in a gas state (g). The corresponding free energy of adding water from S_w into S_m at step i is given by

$$\Delta\Delta G_i^m((i+1)\Delta N_w) = \frac{\Delta G_{w(g\to S_m)}((i+1)\Delta N_w) - \Delta G_{w(g\to S_w)}((i+1)\Delta N_w)}{((i+1)\Delta N_w) + N_P + N_N}, \quad (5)$$

and substituting Eqs. (3) and (4) into Eq. (5), we get

$$\Delta\Delta G_i^m((i+1)\Delta N_w) = \frac{G_m(N_P, N_N, (i+1)\Delta N_w) - (G_m(N_P, N_N, i\Delta N_w) + G_w(\Delta N_w))}{((i+1)\Delta N_w) + N_P + N_N}. \quad (6)$$

The excess free energy of mixing of S_w and S_m for a total of I steps is then the sum of the different $\Delta\Delta G_i^m$'s, i.e.,

$$\Delta G_m^{excess} = \Delta G_m((I+1)\Delta N_w) = \sum_{i=1}^{I} \frac{\Delta G_i^m((i+1)\Delta N_w)}{((i+1)\Delta N_w) + N_P + N_N}. \quad (7)$$

Finally, to get the total free energy of mixing, the ideal free energy of mixing is then added to this excess free energy

$$\Delta G_m^{total} = \Delta G_m^{excess} + \Delta G_m^{ideal}, \quad (8)$$

where the ideal part is estimated simply by

$$\Delta G_m^{ideal} = RT\left[x_w \ln \phi_w + x_{N/P} \ln \phi_{N/P}\right]. \quad (9)$$

Using this methodology to estimate ΔG_m^{total} requires accurate computation of $\Delta G_{w(g\to S_w)}$ and $\Delta G_{w(g\to S_m)}$ from MD simulation at each step. Since the free energy difference of adding water molecules from gas to bulk water, $\Delta G_{w(g\to S_w)}$, is constant at every addition step, only one free energy calculation is needed for the pure water system. However, in the case of S_m, the value of $\Delta G_{w(g\to S_m)}$ would vary at each step due to the change in physical properties of the water/NMP/PVDF system with increasing water concentration. However, we do not need to calculate $\Delta G_{w(g\to S_m)}$ at every water-addition step ranging from pure PVDF/NMP ($\phi_w = 0$) to a pure water state ($\phi_w = 1$) if the increase in the concentration is satisfactorily small. Thus, a linear change in $\Delta G_{w(g\to S_m)}$ is assumed to evaluate the subsequent concentration point (Fig. 2) since the increase in the concentration is small here. In the present study, the free energy calculation of adding water molecules is done for two different starting concentrations of the PVDF/NMP system ($\phi_P = 0.05$ and 0.1), shown in Fig. 2, in order to guarantee the quality of our calculation from the statistical point of view. The exact number of molecules in each system is listed in Tables S1 and S2 in the supplementary material. Note that the concentration of water is only increased up to a maximum of $\phi_w = 0.55$ because the phase separation point is expected to be located at low ϕ_w.

Construction of co-existing phases from MD

Generally, whether a polymer can mix with solvent or nonsolvent depends on the sign of ΔG_m. Mixing is favorable if $\Delta G_m > 0$

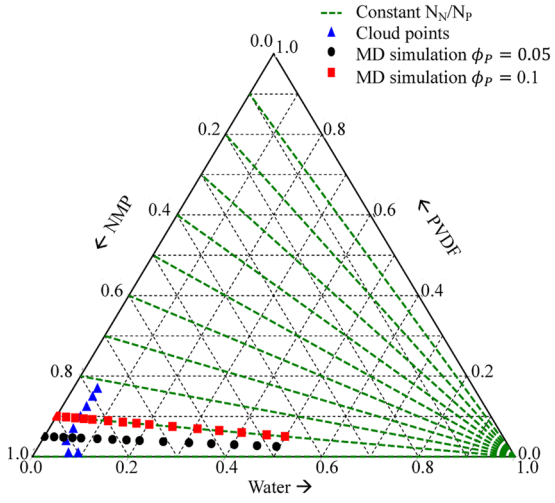

FIG. 2. Ternary phase diagram showing the composition of PVDF solutions (in volume fraction) at which the free energy simulations were carried out (black dots and red squares). The experimental cloud points are taken from the work of Ghodsi *et al.*[26]

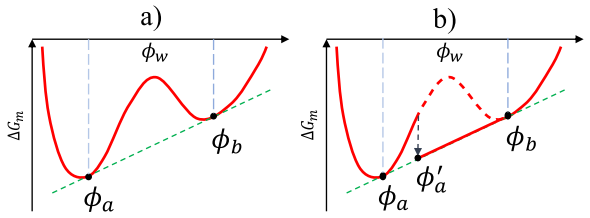

FIG. 3. Schematic diagram for common tangent construction to find the co-existing phases. Shown is a sketch of free energy of mixing, ΔG_m, vs volume fraction, ϕ_w (red solid curve), and a common tangent (green dash line) to two concentration values (blue dashed lines): (a) for a real system and (b) for a molecular dynamics simulation system.

and unfavorable if $\Delta G_m < 0$. However, this criterion alone is not sufficient to know if a polymer mixture is truly stable against separation into two phases. To predict the phase behavior of polymer solutions, we need to study the shape of the curve of ΔG_m as a function of the mixture composition. One way to determine the concentration at which two phases can co-exist is by constructing the common tangent to two minima of ΔG_m, as schematically shown in Fig. 3(a). This is an elegant approach to predict the phase separation point of multicomponent systems, which ensures that the chemical potential for all the components in the two phases is equal. Thermodynamically, increasing the concentration from $\phi_w = 0$, homogeneously mixed solutions at low values of ϕ_w show a phase separation point when $\phi_w = \phi_a$, where two phases with ϕ_a and ϕ_b are observed. However, in the MD calculations, a homogeneously mixed solution is found at values of higher than ϕ_a and phase separation occurs when $\phi_w = \phi'_a$, as shown in Fig. 3(b). This is caused by two factors. The first one is the metastability of the homogeneous system naturally observed even in a real system. The second is the finite size effect, that is, the small system in the periodic boundary condition. In this case, even unstable state may appear in the calculation. A typical example of such behavior is a van der Waals loop found for the MD result of the Lennard Jones (LJ) fluids on the gas-liquid phase transition. Nevertheless, we can evaluate ΔG_m by utilizing the homogenously mixed systems in the MD simulation up to ϕ'_a. The calculated value of ΔG_m would then give the thermodynamically correct phase transition point by constructing a common tangent, as shown in Fig. 3(b), despite the overshoot in phase separation.

Molecular dynamics simulation protocol

For this research, all-atom MD simulations of pure, binary, and ternary systems of PVDF(50-mer), NMP, and water were carried out at various concentrations in order to estimate the free energy of mixing and predict the phase behavior of such systems. The systems were constructed using the Lachet *et al.*[27] force field for PVDF, the Gontrani *et al.*[28] force field for NMP, and the TIP4P/2005 water model.[29] This choice of water model is because the TIP4P/2005 model is best at reproducing the experimental density profile of water/NMP systems when compared to other common water models (TIP4P/EW[30] and TIP3P[31]). The density profile from our MD simulations of the NMP/water system with increasing mole fraction of NMP (x_N) is shown in Fig. S1 in the supplementary material for the three different water models.

For all the systems simulated, each initial configuration was generated by randomly arranging the molecules in a cubic box. The system was then energy minimized using the steepest decent method and equilibrated in a canonical ensemble (NVT) and subsequently in an isothermal–isobaric (NPT) ensemble. After equilibration simulations, a production MD run was conducted in an NPT ensemble, maintaining the temperature at 298 K with a Nose-Hoover thermostat with a coupling time of 0.1 ps. Isotropic pressure coupling was implemented using the Parrinello–Rahman barostat with a reference pressure of 1 bar and a coupling time of 1.0 ps. Furthermore, a time step of 2 fs was employed, and bonds were constrained using the LINear Constraint Solver (LINCS) algorithm. Long-range electrostatic interactions were calculated using the particle mesh Ewald (PME) summation with a Fourier spacing of 0.12 nm and fourth-order interpolation. The van der Waals and Coulomb cutoff were set to 1.2 nm. All the simulations were performed using GROMACS 5.1.4 MD package.[32]

The methodology applied to quantify the free energy change when adding water from the gaseous state into the PVDF solution, $\Delta G_{w(g\to S_m)}$, and into pure water, $\Delta G_{w(g\to S_w)}$, is described in detail in the supplementary material.

RESULTS AND DISCUSSION

Snapshots of the final state of the MD simulations of water/NMP/PVDF at the composition shown in Fig. 2 are presented in Fig. 4. As expected, the PVDF is uniformly distributed in pure NMP and at low concentrations of water. With increasing water

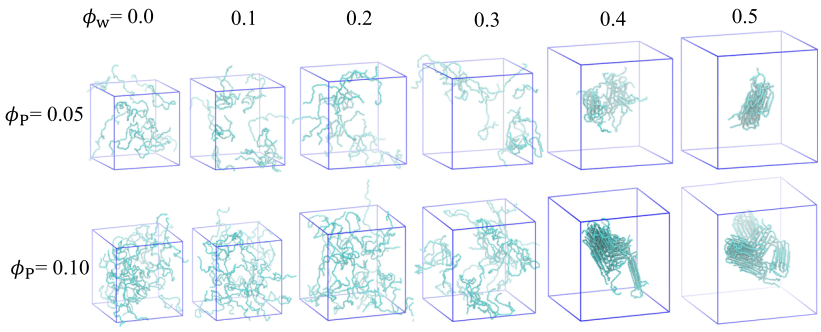

FIG. 4. Final simulation snapshots of water/NMP/PVDF systems at increasing volume fractions of water, ϕ_w, for two different initial concentrations of PVDF/NMP (ϕ_P = 0.05 and ϕ_P = 0.1). For clarity, water and NMP molecules are omitted.

concentration, association of PVDF can be clearly seen in the solution due to the hydrophobic nature of PVDF. It is interesting to note that very similar distributions of PVDF are observed for the two sets of simulations (ϕ_P = 0.05 and ϕ_P = 0.1). This is because the phase transition point is not sensitive to the concentration of PVDF since the cloud point is around ϕ_w = 0.05 for all values of ϕ_P.[26] For ϕ_w > 0.4, complete phase separation of PVDF, i.e., solid-liquid demixing accompanied with crystallization, is obtained in both sets of simulation. This phase separation point is greater than the experimental cloud point ϕ_w = 0.05, as demonstrated in Fig. 3(b), due to the small size of the system and periodic boundary condition.

To assess the structural changes in PVDF in NMP/water, its persistence length, l_p, was calculated (Fig. 5). l_p is a measure of the chain stiffness defined as the length at which the tangents at two points along a polymer chain become decorrelated. This can be measured by considering the autocorrelation of bond vectors at increasing separation, given by

$$C(n) = \langle \cos\theta_{i,i+n} \rangle = \left\langle \frac{\mathbf{a}_i \cdot \mathbf{a}_{i+n}}{|\mathbf{a}_i||\mathbf{a}_{i+n}|} \right\rangle, \tag{10}$$

where $C(n)$ measures the correlation of bond i with bonds along the backbone, with $\mathbf{a}_i$ representing the bond as a vector. Angular brackets represent an average over all possible start points in all chains. This correlation function is then fitted to an exponential equation

$$C(n) \approx \exp\left(-\frac{x}{l_p}\right), \tag{11}$$

where fitting parameter l_p is the persistence length.

As can be seen, the value of l_p remains almost constant at low ϕ_w and increases rapidly at ϕ_w > 0.3 for ϕ_P = 0.05 and ϕ_w > 0.35 for ϕ_P = 0.1. This rise in l_p indicated that PVDF becomes stiffer when increasing the concentration of water due to the crystallization of PVDF upon association, which is clearly seen in the simulation snapshots.

A similar trend as l_p is seen when studying the PVDF-PVDF interaction energy (Fig. 6), calculated as the sum of the PVDF-PVDF

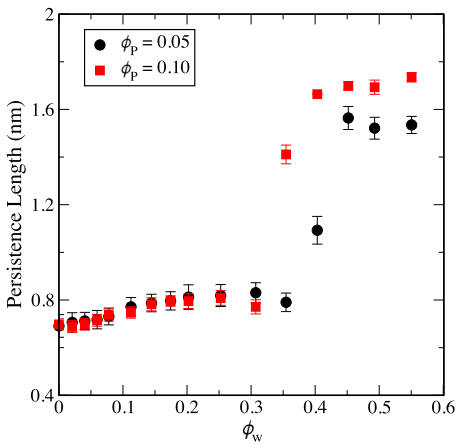

FIG. 5. The persistence length of PVDF in NMP and water with increasing volume fraction of water (ϕ_w).

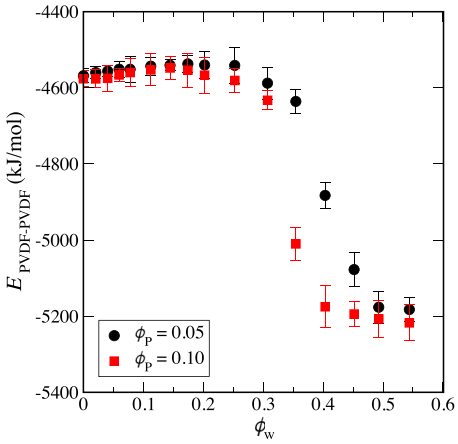

FIG. 6. PVDF-PVDF intermolecular interaction energy, $E_{PVDF-PVDF}$, as a function of water volume fraction, ϕ_w, for two different initial PVDF/NMP system compositions (volume fraction of PVDF ϕ_P = 0.05 and 0.1).

LJ and Coulomb potential energy. As can be seen, a slight increase in the PVDF-PVDF interaction energy occurs with increasing values of ϕ_w. Upon further addition of water, the strength of the PVDF-PVDF interaction rapidly increases for both sets of simulations due to the association of PVDF molecules. However, a slightly stronger PVDF-PVDF interaction is found for ϕ_P = 0.1 which explains the shift to the left in the rapid rise of l_p. The clear discontinuity of the trend in the structural and energetic properties of PVDF found at around ϕ_w = 0.3 for ϕ_P = 0.05 and ϕ_w = 0.35 for ϕ_P = 0.1 indicates a phase transition. This must represent the MD phase separation point, i.e., ϕ_a' in Fig. 3(b), from the homogenously mixed solution to the phase separated solid/liquid phase. This is in correspondence to the observation in Fig. 4 where the aggregated polymer chains are produced at that concentration. Furthermore, this result agrees with the fact that, experimentally, precipitation of PVDF occurs when water is added to the PVDF/NMP solution. In the section titled "Free energy of mixing from MD simulation," we estimate the thermodynamic phase separation point through calculation of ΔG_m^{MD}, which is equivalent to the experimental cloud point.

Free energy of mixing from MD simulation

To provide a deeper understanding into the miscibility of water/NMP/PVDF, the free energy of mixing and the thermodynamic phase separation point were estimated as described in the section titled "Methodology." First, the $\Delta G_{w(g\to S_w)}$ was estimated as −30.476 kJ/mol by taking the average of three independent calculations with a different number of water molecules in system S_w. These values, along with their errors, are listed in Table I. The estimated values show that the free energy calculation is independent of the system size. Furthermore, the average value of $\Delta G_{w(g\to S_w)}$ is very close to previous calculations in the literature (−28 kJ/mol for SPC water model by Riniker *et al.* and −27 kJ/mol by Marrink *et al.*).[33,34]

Following the same procedure, $\Delta G_{w(g\to S_m)}$ was estimated with increasing values of ϕ_w for the two sets of systems with different

TABLE I. The free energy change upon adding water from the gas state (*g*) to the bulk of water (system S_w), $\Delta G_{w(g\to S_w)}$, with increasing number of water molecules, N_w, in S_w. The standard errors are estimated from average variance of 5 blocks each with 10 ns length.

N_w in S_w	$\Delta G_{(g\to G_w)}$ (kJ/mol)	Error
1600	−30.46	0.05
10000	−30.49	0.04
34000	−30.48	0.11
Average	−30.476	0.20

starting concentrations of PVDF (Fig. 7). The results show that all concentrations of water give negative values of $\Delta G_{w(g\to S_m)}$, indicating that it is more favorable for water molecules to be in the PVDF solution than in the gas state. Less negative values are obtained for the higher concentration of PVDF ($\phi_P = 0.1$), making it slightly less favorable for water to be dissolved in the PVDF solution due to the hydrophobic nature of PVDF. Additionally, it is found that the $\Delta G_{w(g\to S_m)}$ values are lower than that of $\Delta G_{w(g\to S_w)}$, which means the water molecules are more thermodynamically stable in pure water than in the PVDF solution. When analyzing the $\Delta G_{w(g\to S_m)}$ profile with increasing volume fraction of water, both sets of calculations show that the value increases up to concentrations $\phi_w = 0.17$ and then decreases again for $\phi_w > 0.17$. Again, this turning point relates to the change in the thermodynamic phase property of the PVDF solution with increasing composition of water. However, the point at which the maximum is observed from this calculation is at much lower value of ϕ_w than the point at which the PVDF-PVDF intermolecular interaction energy decreases sharply, shown in Fig. 6. Furthermore, it is interesting to find a slight drop in the value of $\Delta G_{w(g\to S_m)}$ at $\phi_w = 0.3$ for $\phi_P = 0.05$, which is due to the solid/liquid phase separation, clearly observed in the simulation snapshots (Fig. 4). However, this is not seen for the higher

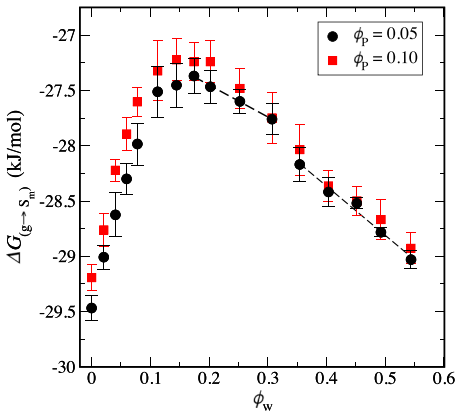

FIG. 7. The free energy change upon adding water from the gas state (*g*) to system S_m, $\Delta G_{w(g\to S_m)}$, against volume fraction of water ϕ_w for two different initial concentrations of PVDF/NMP system (volume fraction of PVDF $\phi_P = 0.05$ and 0.1). The dashed black lines are the linear regressions for sections $\phi_P = 0.05$ data.

concentration of PVDF simulations, $\phi_P = 0.1$. The failure to clearly capture the transition to the solid/liquid phase in the $\Delta G_{w(g\to S_m)}$ profile might be due to the small change in the $\Delta G_{w(g\to S_m)}$ value with increasing ϕ_w and the error associated with the calculation.

Implementing Eq. (7), ΔG_m^{excess} was then estimated [Fig. 8(a)] for the two sets of systems. Looking at the plot of ΔG_m^{excess}, a positive value is obtained for all the compositions, with the value increasing with the increasing volume fraction of water, due to the hydrophobicity of PVDF. However, for the system with higher PVDF concentration ($\phi_P = 0.1$), ΔG_m^{excess} increases with a steeper gradient. Estimating the first derivative of ΔG_m^{excess} with respect to ϕ_w [Fig. 8(b)], we can clearly see an inflection point at $\phi_w = 0.11$ for both cases, across which the ΔG_m^{excess} profile changes its curvature from convex to concave. This is closely related to the presence of co-tangent curves, representing a phase transition.

Further insight into the miscibility of this system can be achieved by decomposing the excess free energy of mixing into entropic and enthalpic terms. The enthalpic term can be estimated by considering the potential energy change from the PVDF/NMP and water system to the PVDF/NMP/water mixed system from MD simulations as

$$\Delta H_m = E_m - \left(x_w E_w + x_{N/P} E_{N/P}\right). \tag{12}$$

Here, E_m, $E_{N/P}$ and E_w stand for the potential energy of the mixed water/NMP/PVDF and NMP/PVDF systems, and the neat water system, respectively. Then, the entropy of mixing can simply be calculated as

$$-T\Delta S_m = \Delta G_m - \Delta H_m. \tag{13}$$

Applying these equations, the estimated values of $\Delta H_m^{excess} (= \Delta H_m)$ and $-T\Delta S_m^{excess}$ along with ΔG_m^{excess} are plotted in Fig. 9. Mixing PVDF/NMP with water is enthalpically favorable (negative value) for all the concentrations studied, with a minimum value at $\phi_w = 0.17$ for both sets of calculations. With regard to the excess entropy of mixing, it is clear that the miscibility of PVDF/NMP with water is entropically unfavorable and the value of $-T\Delta S_m^{excess}$ increases with increasing concentration of water. This correlates with the large reduction in the conformational and translational entropy of PVDF, in particular, when self-association and phase separation occur in the solution. The contribution of the $-T\Delta S_m^{excess}$ term to the excess free energy of mixing exceeds the value of ΔH_m with increasing concentration of water. Thus, based on ΔG_m^{excess}, the unfavorable miscibility of the PVDF/NMP with water across the composition range is of entropic origin. Crucially, the finding of nonzero values of $-T\Delta S_m^{excess}$ of such mixtures contradicts the approximation made in the FH theory. In the extended FH theory, the presence of excess entropy is normally lumped into the temperature-dependent χ, which arises from the volume change upon mixing and local packing. Empirically, the temperature dependence of χ is often written as a sum of two terms

$$\chi(T) = A + \frac{B}{T}, \tag{14}$$

where A is referred to as the "entropic part" and B/T is referred to as the "enthalpic part" of χ. However, the parameters A and B are mainly estimated for polymer blends since they show clear

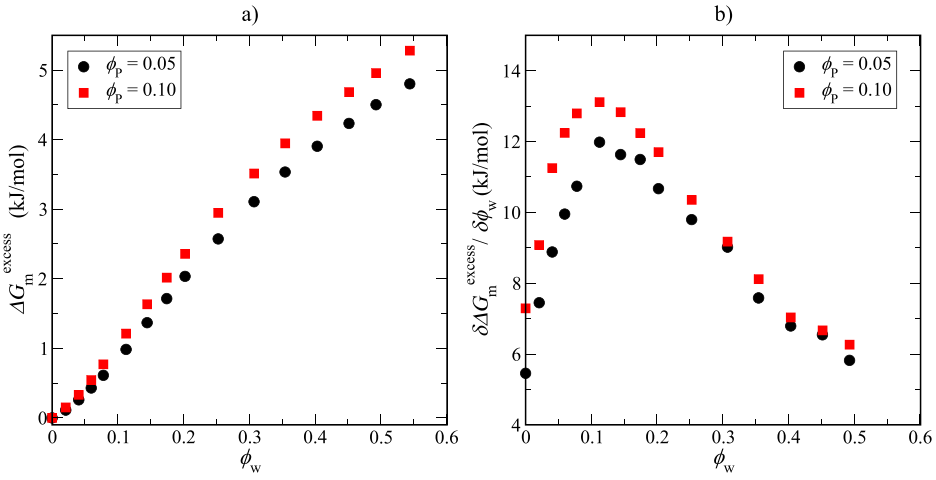

FIG. 8. (a) The excess free energy of mixing, ΔG_m^{excess}, of the water/NMP/PVDF system with increasing volume fraction of water (ϕ_w). (b) The approximate first derivative of ΔG_m^{excess} with respect to ϕ_w.

volume change upon mixing. Our result shows that even for a polymer solution, the excess entropy term is significant in the free energy of mixing estimation. This will be discussed in detail in the section titled "The Flory-Huggins free energy of mixing."

Next, we look at ΔG_m^{total} of the water/NMP/PVDF system with increasing concentrations of water, calculated by summing ΔG_m^{excess} and ΔG_m^{ideal}. Figure 10 depicts the estimated composition dependence of ΔG_m^{total}, along with ΔG_m^{excess} and ΔG_m^{ideal}. In the case of ΔG_m^{ideal}, since ideal entropy always acts to promote mixing, a negative value is found for all compositions, with a minimum value at $\phi_w = 0.175$. However, this analysis was only done up to $\phi_w = 0.3$ since the ideal mixing entropy equation can only be applied for homogeneously mixed systems. The calculated value of ΔG_m^{total} becomes negative at low concentrations, with a minimum at about 0.07 volume fraction of water for both the $\phi_P = 0.05$ and 0.1 systems. As mentioned above, prediction of the phase separation point of the water/NMP/PVDF system can be achieved by studying the free energy of mixing profile and constructing the common tangent. However, in our estimation of ΔG_m^{total}, a second minimum is not observed due to the difficulty in estimating $\Delta G_{w(g\rightarrow S_m)}$ at higher concentrations of water. Instead, a tangent line to the ΔG_m^{total} curve that intersects the point $\phi_w = 1$ and $\Delta G_m^{total} = 0$ is drawn, as shown in Fig. 10, because we expect the second minimum to be located closer to $\phi_w = 1$. By doing this, the thermodynamic phase separation point is found to be at $\phi_w = 0.08$ for both concentrations of PVDF, in good agreement with the experimental cloud point value, $\phi_w = 0.05$.[26] The slight discrepancy is most likely from the difference in the degree of polymerization of the PVDF since the calculations use a 50-mer, whereas the real PVDF has, on average, 3000 monomers.

Applying the estimates of ΔH_m above, ΔG_m^{total} was then decomposed into entropic and enthalpic terms using Eq. (13), as shown in

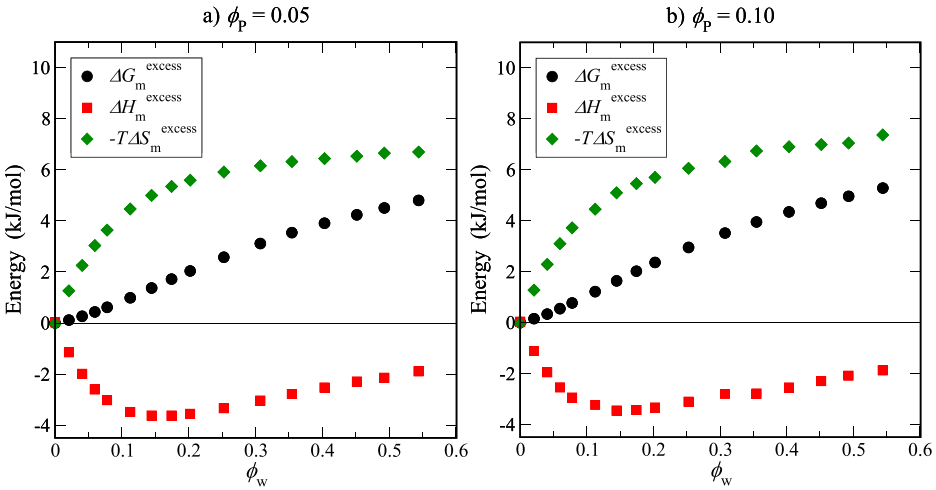

FIG. 9. Decomposition of the excess free energy of mixing, ΔG_m^{excess}, of the water/NMP/PVDF system into excess entropy of mixing ($-T\Delta S_m^{excess}$) and excess enthalpy of mixing (ΔH_m^{excess}). (a) Volume fraction of PVDF $\phi_P = 0.05$ and (b) $\phi_P = 0.1$ for the initial concentration of the PVDF/NMP system.

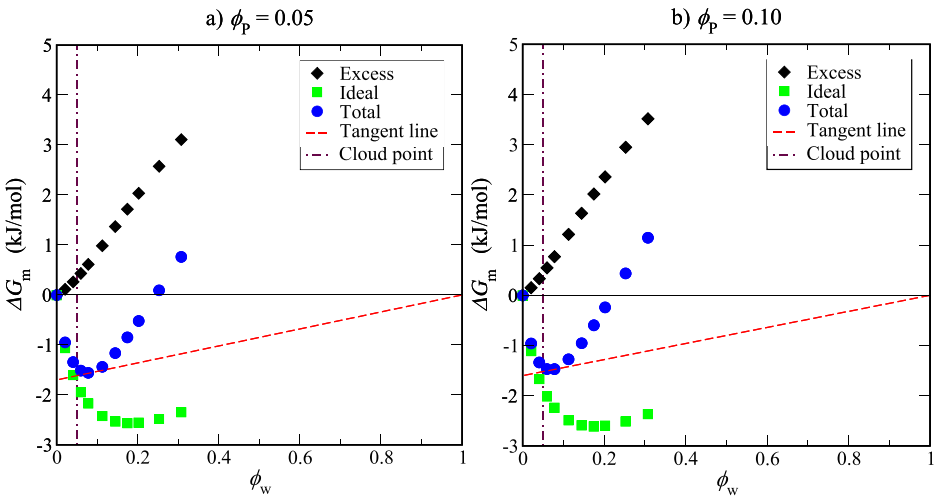

FIG. 10. ΔG_m^{total}, ΔG_m^{excess}, and ΔG_m^{ideal} of the water/NMP/PVDF system with increasing concentration of water for two different initial concentrations of the PVDF/NMP system. (a) Volume fraction of PVDF $\phi_P = 0.05$ and (b) $\phi_P = 0.1$. The red dotted line is the tangent line to the ΔG_m^{total} curve, which intersects the point $\phi_w = 1$ and $\Delta G_m^{total} = 0$.

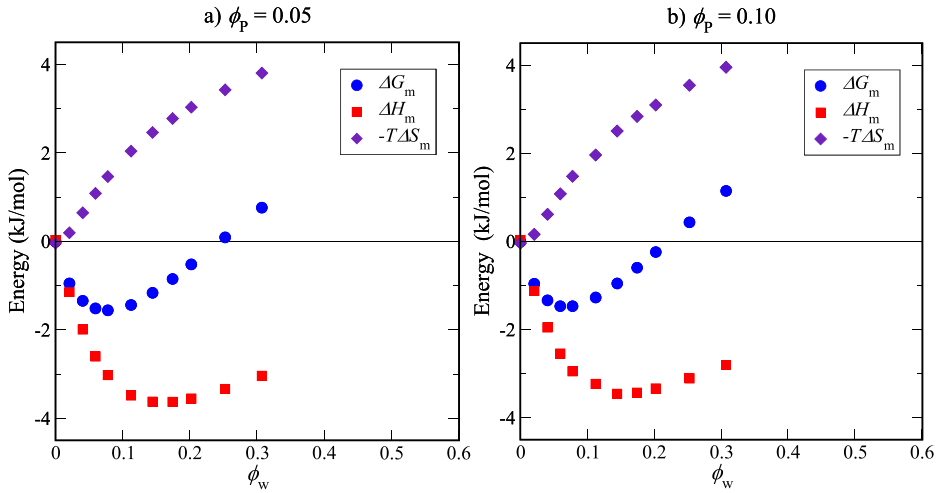

FIG. 11. Decomposition of the total free energy of mixing, ΔG_{mix}^{total}, of the water/NMP/PVDF system to the enthalpy of mixing, ΔH_m, and entropy of mixing, $-T\Delta S_m$, with increasing volume fraction of water, ϕ_w. (a) Volume fraction of PVDF $\phi_P = 0.05$ and (b) $\phi_P = 0.1$ for the initial concentration of the PVDF/NMP system.

Fig. 11. At low concentrations of water, the enthalpy of mixing has a much more significant contribution than entropy of mixing on the miscibility of the ternary system. However, with increasing concentrations of water, the contribution from the enthalpic term reduces and the entropic component dominates. This tells us that the immiscibility of PVDF as a result of water addition in the polymer solution is of entropic origin at higher concentrations of water.

The Flory-Huggins free energy of mixing

In this section, we compare the calculated values of ΔG_m^{MD} with the FH theory, which is a very popular and easy to use theory, although little has been discussed about its validity for quantitative prediction. Estimating the free energy of mixing based on the FH theory requires the computation of the binary interaction parameters χ_{ij} for all pairs of components. Atomistic MD simulations can be used in the framework of FH theory to estimate the concentration-dependent interaction parameters between two components i and j by applying the equation[35,36]

$$\chi_{ij} = \frac{V_{ref}\Delta H_m}{RTV_m\phi_i\phi_j}, \tag{15}$$

where V_{ref} is the reference volume, which is taken to be the average volume of the PVDF monomer, V_m is the total volume of the mixture, and ΔH_m is the enthalpy change upon mixing. From MD simulations of pure and mixed binary component systems at different concentrations, the value of $\Delta H_m/V_m$ can be estimated by calculating the cohesive energy densities of the mixed (CED_m) and pure systems (CED_i and CED_j) as

$$\begin{aligned}\frac{\Delta H_m}{V_m} &= CED_m - \left(CED_i\phi_i + CED_j\phi_j\right)\\ &= \left(\frac{\Delta E_{coh}}{V}\right)_m - \left[\left(\frac{\Delta E_{coh}}{V}\right)_i\phi_i + \left(\frac{\Delta E_{coh}}{V}\right)_j\phi_j\right],\end{aligned} \tag{16}$$

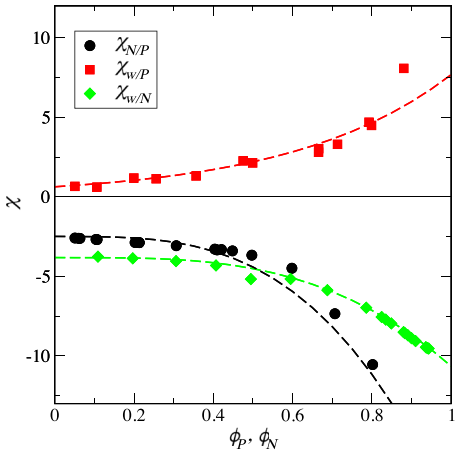

FIG. 12. Concentration dependence of interaction parameters for NMP/PVDF ($\chi_{N/P}$) and water/PVDF ($\chi_{w/P}$) with increasing volume fractions of PVDF (ϕ_P) and for water/NMP ($\chi_{w/N}$) with increasing volume fractions of NMP (ϕ_N). The dashed lines are the fitted functions listed in shown Table II.

where V is volume of the system and

$$\Delta E_{coh} = E_{system} - \sum_i n_i E_i. \tag{17}$$

The values of E_{system}, n_i, and E_i denote the energy of a bulk system, the number of component molecules, and the energy of a single component molecule in vacuum, respectively. Once the concentration-dependent $\chi_{w/N}$, $\chi_{N/P}$, and $\chi_{w/P}$ are estimated using the above methodology, the value of ΔG_m^{FH} at any concentration of the three components can be obtained using Eq. (1). From this, the ternary phase diagram of nonsolvent/solvent/polymer can be constructed by calculating the binodal and spinodal curves along the tie-lines.[37,38]

TABLE II. Flory-Huggins interaction parameters of water/NMP, NMP/PVDF, and water/PVDF. Case 1 takes all χ_{ij}'s as constants, whereas case 2 considers the concentration-dependent χ_{ij}'s.

1	2
$\chi_{w/N} = -9.32$	$\chi_{w/N}(u_N) = -8.414u_N^3 + 1.75u_N^2 - 0.16u_N - 3.82$
$\chi_{N/P} = -2.60$	$\chi_{N/P}(\phi_P) = -20.11\phi_P^3 - 2.88\phi_P^2 + 0.26\phi_P - 2.49$
$\chi_{w/P} = 0.52$	$\chi_{w/P}(\phi_P) = 0.63e^{2.5\phi_P}$

The concentration-dependent χ_{ij} of PVDF/NMP, PVDF/water, and NMP/water were quantified from the simulation results using the cohesive density approach, and the results are presented in Fig. 12. Consistent with the simulation images of binary systems presented in Fig. S2, the χ_{ij} results show that PVDF and NMP are mutually soluble (negative $\chi_{N/P}$), while PVDF and water are insoluble (positive $\chi_{w/P}$) for all volume fractions. Additionally, negative values of $\chi_{w/N}$ occur for all concentrations, indicating that mixing is favorable and all the solution compositions are stable. More importantly, our results show that there is a very clear composition dependency of χ_{ij}, with a noticeable increase for PVDF/water and decrease for PVDF/NMP and NMP/water when $\phi > 0.6$. However, in the literature, the NMP/PVDF and water/PVDF interaction parameters are normally calculated from solubility parameters and are taken as constant values ($\chi_{N/P} = 0.35$ and $\chi_{w/P} = 2.6$).[4]

To compare ΔG_m^{MD} with the FH model, ΔG_m^{FH} was calculated for the same concentrations of water/NMP/PVDF as shown above. Furthermore, the influence of using constant χ_{ij} vs concentration dependent χ_{ij} on the free energy of mixing was evaluated using two sets of χ_{ij} parameters, listed in Table II. The first set has constant χ_{ij}, with the values taken from the calculated χ_{ij} at ϕ_N and ϕ_P equal to 0.9 and 0.1, respectively. The second set is the concentration-dependent χ_{ij} expression found by fitting a polynomial or exponential function to the calculated data points. Figure 13 illustrates

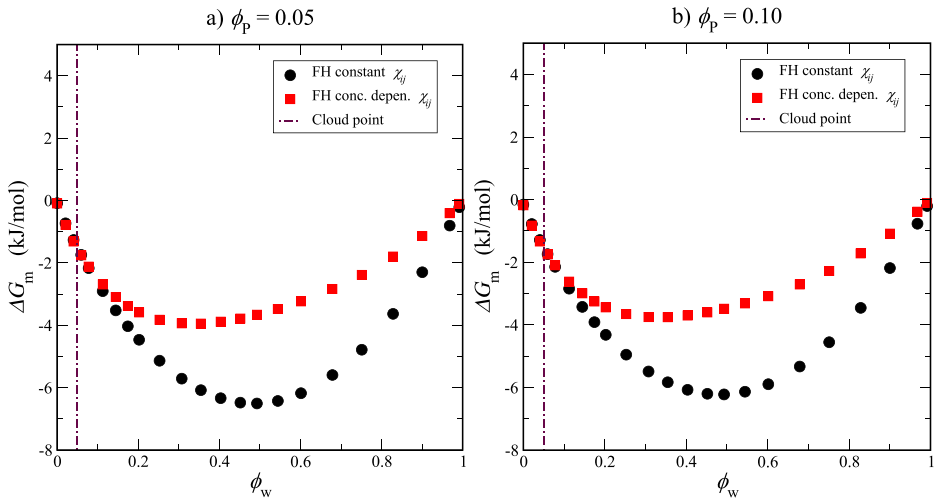

FIG. 13. Composition dependent FH free energy of mixing using constant and concentration dependent interaction parameter χ_{ij}. (a) Volume fraction of PVDF ϕ_P = 0.05 and (b) ϕ_P = 0.1 for the initial concentration of the PVDF/NMP system.

the values of ΔG_m^{FH} calculated using these two sets of χ_{ij} parameters. It can be seen that ΔG_m^{FH} follows a convex curve for both constant and concentration-dependent interaction parameters. This means that the FH model predicts the PVDF solution to be a stable homogeneous mixture across the whole concentration range. The MD simulations demonstrate that this is definitely not the case. This tells us that even implementing the concentration-dependence of χ_{ij} still gives unrealistic ΔG_m^{FH} profiles. The failure of the FH model to accurately predict the thermodynamic phase behavior of the PVDF solution is largely because it does not consider the ternary interactions and the excess entropy of mixing. As we have clearly shown in the section titled "Free energy of mixing from MD simulation," the excess entropic term has significant contribution to the free energy of mixing of water/NMP/PVDF.

CONCLUSION

The thermodynamic phase behavior of water/NMP/PVDF has been investigated through all-atom MD calculation by estimating the free energy of mixing of the PVDF/NMP solution with water for increasing water concentrations. In this work, an accurate approach, beyond the classical FH theory, is applied to determine the free energy of mixing, which incorporates the ternary interaction of water/NMP/PVDF as well as the full enthalpic and entropic terms of the free energy of mixing. The thermodynamic phase separation points of the ternary system were predicted to be at $\phi_w = 0.08$ for the two sets of calculation with different concentrations of PVDF, in good agreement with the experimental cloud point measurement, $\phi_w = 0.05$. We would like to stress that this calculation gives a satisfactory value for the free energy of mixing, even for the NIPS process, i.e., phase separation of polymer induced by spontaneous mixing of nonsolvent with a polymer solution. Decomposition of the total free energy of mixing into the entropic and enthalpic term revealed that at low concentrations of water, the contribution from the enthalpic term is more important, but at higher concentrations of water, the entropic contribution dominates, becoming more unfavorable with increasing concentration of water.

For comparison, the FH free energy of mixing was estimated based on concentration-dependent χ_{ij} from binary MD simulations of PVDF/NMP, PVDF/water, and NMP/water. Contrary to the ternary MD simulation trajectory results and the free energy of mixing from MD calculation, the FH theory predicted the PVDF solution to be a homogeneous stable mixture across the concentration range studied. The greatest shortage of the FH model is the fact that the excess entropy of mixing is neglected.

We conclude by noting that the free energy of mixing calculation for a nonsolvent/solvent/polymer system based on MD calculation is fairly accurate and is efficient in capturing the thermodynamic phase separation point. Improvement of the FH theory can be easily done by converting the free energy of mixing from MD calculations to a form of effective χ_{ij}, which includes the excess entropy term, concentration dependency, as well as the contribution from the ternary interaction at specific temperature. Thus, the accurately estimated χ can be used in mesoscopic simulation software that is based on the standard FH theory. Such a procedure will provide a new way to mesoscopically simulate the NIPS process in a more realistic manner, such as density functional theory self-consistent field (DFT-SCF).[39]

In future work, we will try to reveal the microscopic origin of the thermodynamic phase behavior of the water/NMP/PVDF ternary system for the full PVDF concentration space. Additionally, we will try to perform mesoscopic simulation for the NIPS process using an effective χ_{ij} which gives the correct free energy of mixing.

SUPPLEMENTARY MATERIAL

See supplementary material for detailed description of the methodology for calculating the free energy change when adding water from the gaseous state into the PVDF solution and the exact composition of PVDF solutions at which the free energy simulations were carried out. Also, the density profile of the NMP/water system at various concentrations using three different water models (TIP4P-2005, TIP4P/EW, and TIP3P) is provided.

ACKNOWLEDGMENTS

This paper is based on the research results from a project (Grant No. P16010) commissioned by the New Energy and Industrial Technology Development Organization (NEDO).

REFERENCES

[1] I. Hopkinson and M. Myatt, Macromolecules **35**, 5153 (2002).
[2] H. Strathmann and K. Kock, Desalination **21**, 241 (1977).
[3] S. Mazinani, S. Darvishmanesh, A. Ehsanzadeh, and B. Van der Bruggen, J. Memb. Sci. **526**, 301 (2017).
[4] P. Sukitpaneenit and T.-S. Chung, J. Memb. Sci. **340**, 192 (2009).
[5] H. Tompa, Trans. Faraday Soc. **45**, 1142 (1949).
[6] P. J. Flory, J. Chem. Phys. **10**, 51 (1942).
[7] M. L. Huggins, J. Phys. Chem. **46**, 151 (1942).
[8] A. J. Nedoma, M. L. Robertson, N. S. Wanakule, and N. P. Balsara, Macromolecules **41**, 5773 (2008).
[9] R. G. M. van der Sman, Food Funct. **8**, 360 (2017).
[10] K. Pajula, M. Taskinen, V. P. Lehto, J. Ketolainen, and O. Korhonen, Mol. Pharm. **7**, 795 (2010).
[11] D. R. Tree, K. T. Delaney, H. D. Ceniceros, T. Iwama, and G. H. Fredrickson, Soft Matter **13**, 3013 (2017).
[12] D. R. Tree, T. Iwama, K. T. Delaney, J. Lee, and G. H. Fredrickson, ACS Macro Lett. **7**, 582 (2018).
[13] E. R. Turpin, V. Taresco, W. A. Al-Hachami, J. Booth, K. Treacher, S. Tomasi, C. Alexander, J. Burley, C. A. Laughton, and M. C. Garnett, Mol. Pharm. **15**, 4654 (2018).
[14] B. D. Anderson, J. Pharm. Sci. **107**, 24 (2018).
[15] G. Miquelard-Garnier and S. Roland, Eur. Polym. J. **84**, 111 (2016).
[16] D. Z. Icoz and J. L. Kokini, Carbohydr. Polym. **68**, 59 (2007).
[17] M. Tambasco, J. E. G. Lipson, and J. S. Higgins, Macromolecules **39**, 4860 (2006).
[18] S. Bruckner and S. Boresch, J. Comput. Chem. **32**, 1303 (2011).
[19] F. M. Ytreberg, R. H. Swendsen, and D. M. Zuckerman, J. Chem. Phys. **125**, 184114 (2006).
[20] S. Bruckner and S. Boresch, J. Comput. Chem. **32**, 1320 (2011).
[21] N. Huang, C. Kalyanaraman, K. Bernacki, and M. P. Jacobson, Phys. Chem. Chem. Phys. **8**, 5166 (2006).
[22] Y. Deng and B. Roux, J. Phys. Chem. B **113**, 2234 (2009).
[23] P. Jedlovszky, A. Idrissi, and G. Jancsó, J. Chem. Phys. **130**, 124516 (2009).

[24]A. Idrissi, B. Marekha, M. Barj, and P. Jedlovszky, J. Phys. Chem. B **118**, 8724 (2014).
[25]C. H. Bennett, J. Comput. Phys. **22**, 245 (1976).
[26]A. Ghodsi, H. Fashandi, M. Zarrebini, M. M. Abolhasani, and M. Gorji, RSC Adv. **5**, 92234 (2015).
[27]V. Lachet, J. M. Teuler, and B. Rousseau, J. Phys. Chem. A **119**, 140 (2015).
[28]L. Gontrani and R. Caminiti, J. Chem. Phys. **136**, 074505 (2012).
[29]J. L. F. Abascal and C. Vega, J. Chem. Phys. **123**, 234505 (2005).
[30]H. W. Horn, W. C. Swope, J. W. Pitera, J. D. Madura, T. J. Dick, G. L. Hura, and T. Head-Gordon, J. Chem. Phys. **120**, 9665 (2004).
[31]W. L. Jorgensen, J. Chandrasekhar, J. D. Madura, R. W. Impey, and M. L. Klein, J. Chem. Phys. **79**, 926 (1983).
[32]S. Pronk, S. Páll, R. Schulz, P. Larsson, P. Bjelkmar, R. Apostolov, M. R. Shirts, J. C. Smith, P. M. Kasson, D. van der Spoel, B. Hess, and E. Lindahl, Bioinformatics **29**, 845 (2013).
[33]S. Riniker and W. F. van Gunsteren, J. Chem. Phys. **134**, 084110 (2011).
[34]S. J. Marrink, H. J. Risselada, S. Yefimov, D. P. Tieleman, and A. H. de Vries, J. Phys. Chem. B **111**, 7812 (2007).
[35]T. M. Madkour, Chem. Phys. **274**, 187 (2001).
[36]M. Ali Mohammad, K. Poulose Santo, S. K. Dew, and M. Stepanova, J. Vac. Sci. Technol. B **30**, 06FF11 (2012).
[37]F. W. Altena and C. A. Smolders, Macromolecules **15**, 1491 (1982).
[38]C. C. Hsu and J. M. Prausnitz, Macromolecules **7**, 320 (1974).
[39]T. Honda and T. Kawakatsu, Macromolecules **40**, 1227 (2007).